

1 Airborne Observations of IEPOX-Derived Isoprene SOA in 2 the Amazon during SAMBBA

3

4 James D. Allan^{1,2}, William T. Morgan¹, Eoghan Darbyshire¹, Michael J. Flynn¹,
5 Paul I. Williams^{1,2}, David E. Oram³, Paulo Artaxo⁴, Joel Brito⁴, James D. Lee⁵,
6 and Hugh Coe¹

7 [1]{School of Earth, Atmospheric and Environmental Sciences, University of Manchester,
8 UK}

9 [2]{National Centre for Atmospheric Science, University of Manchester, UK}

10 [3]{Centre for Ocean and Atmospheric Sciences & National Centre for Atmospheric Science,
11 School of Environmental Sciences, University of East Anglia, Norwich, UK}

12 [4]{Physics Institute, University of São Paulo, Brazil}

13 [5]{Department of Chemistry & National Centre for Atmospheric Science, University of
14 York, UK}

15 Correspondence to: J. D. Allan (james.allan@manchester.ac.uk)

16

17 Abstract

18 Isoprene is a potentially highly significant but currently poorly quantified source of secondary
19 organic aerosols (SOA). This is especially important in the tropics, where large rainforests act
20 as significant sources of isoprene. Methylfuran, produced through thermal decomposition
21 during analysis, has recently been suggested as a marker for isoprene SOA formation through
22 the isoprene epoxydiol (IEPOX) route, which mostly occurs under low NO_x conditions. This
23 is manifested as a peak at $m/z=82$ in Aerodyne Aerosol Mass Spectrometer (AMS) data. Here
24 we present a study of this marker measured during 5 flights over the Amazon rainforest on
25 board the UK Facility for Airborne Atmospheric Measurement (FAAM) BAe-146 research
26 aircraft during the South American Biomass Burning Analysis (SAMBBA) campaign. Cases
27 where this marker is and is not present are contrasted and linked to the presence of acidic seed
28 particles, lower NO_x concentrations and higher humidities. There is also data to suggest a role
29 of organic nitrogen in the particulate composition. Furthermore, an inspection of the vertical

1 trends of the marker indicates that concentrations are highest at the top of the boundary layer
2 (possibly due to semivolatile repartitioning) and upwards through the free troposphere, the
3 mass spectral profile evolves towards that of low volatility oxygenated aerosol. These
4 observations offer insights into the behaviour of IEPOX-derived SOA formation above the
5 Amazon rainforest and the suitability of methylfuran as a marker for this process.

6 **1 Introduction**

7 The processes controlling secondary organic aerosols (SOA) remain a continuing source of
8 uncertainty in our predictive capability of atmospheric composition (Hallquist et al., 2009).
9 These are formed from both natural and anthropogenic precursors and are subject to many
10 complex and often poorly-understood processes that control the formation. Of specific interest
11 in recent years is the formation of SOA from isoprene (Claeys et al., 2004; Carlton et al.,
12 2009; Claeys et al., 2010). Because of isoprene's abundance in the atmosphere, this could
13 represent a significant portion of the SOA budget in certain regions, even if its mass yield is
14 low relative to other natural VOCs such as monoterpenes and sesquiterpenes. While evidence
15 for isoprene SOA formation has existed for some time, laboratory studies have shown that
16 yields are highly variable and dependent on parameters such as NO_x concentrations and the
17 composition of the seed particles (Czoschke et al., 2003). One particular mechanism that has
18 received much attention is through the formation of isoprene epoxydiols (IEPOX) under
19 low-NO_x conditions and reactive uptake to the particle phase, which produces markers that
20 have been observed in the atmosphere such as 2-methyltetrols (Paulot et al., 2009; Chan et al.,
21 2010; Surratt et al., 2010; Surratt et al., 2006; Kroll et al., 2006). The work of Pye et al.
22 (2013) indicates that model representation of these processes can produce the marker
23 compounds in quantities comparable to observations.

24 Another proposed marker is methylfuran, which has been detected using the Aerodyne
25 Aerosol Mass Spectrometer (AMS) and two-dimensional gas chromatography-mass
26 spectrometry analysis of filter samples, first identified by Robinson et al. (2011) in Borneo as
27 part of the Oxidant and Particle Photochemical Processes above a South-East Asian tropical
28 rain forest (OP3) campaign (Hewitt et al., 2010). This is not in itself present in the particles
29 (being too volatile), but is thought to be produced through the decomposition of IEPOX SOA
30 species such as 3-methyltetrahydrofuran-3,4-diols (3-MeTHF-3,4-diols) during the thermal
31 desorption used in both techniques (Lin et al., 2012). Methylfuran is a particularly useful
32 marker because it produces a distinctive signal in the AMS mass spectrum at $m/z=82$. While

1 the majority of the mass is contained within other peaks, these are common to many other
2 forms of SOA and are therefore unsuitable for marker-based analysis. Normally, this peak
3 constitutes no more than 4 % of the organic signal, so a higher fraction can be seen as
4 evidence of the marker being present. While the majority of the mass is contained within
5 other peaks (Robinson et al., 2011; Kiendler-Scharr et al., 2012), these are common to many
6 other forms of SOA and are therefore unsuitable for marker-based analysis. Furthermore, this
7 marker can also form the basis of a factor obtained using Positive Matrix Factorisation (PMF)
8 (Ulbrich et al., 2009), which allows the total amount of organic matter covariant with this
9 marker to be quantified. This can then be used as an estimate of isoprene SOA formed under
10 these conditions, not just that which gives rise to the methylfuran marker. This will also apply
11 to the analysis of data from the Aerosol Chemical Speciation Monitor (ACSM), an instrument
12 similar in function to the AMS but more optimised for long-term monitoring (Ng et al., 2011).

13 This marker has now been reported in a number of environments using ground-based AMS
14 and ACSM measurements, for example in Canada (Slowik et al., 2011) and downtown
15 Atlanta, GA (Budisulistiorini et al., 2013), consistent with the formation of isoprene SOA
16 through the IEPOX route, although not enough data currently exists to form a universal
17 picture of its behaviour. Tropical environments are of particular interest because of the
18 dominance of isoprene in the biogenic VOC budgets (Guenther et al., 2006) and the often
19 lower anthropogenic influence, resulting in lower NO_x concentrations. To date, the $m/z=82$
20 marker has been reported from ground- and aircraft-based measurements in Borneo and
21 ground-based measurements in the Amazon (Chen et al., 2009; Chen et al., 2014). Here we
22 present, for the first time, airborne measurements of this marker above the Amazon. The
23 measurements were performed as part of the South AMERICAN Biomass Burning Analysis
24 (SAMBBA) campaign in 2012, using the Facility for Airborne Atmospheric Measurements
25 (FAAM) BAe-146 research aircraft, with a similar instrument payload as used in Robinson et
26 al. (2011).

27 **2 Experimental**

28 **2.1 Flight Details**

29 While the primary focus of the SAMBBA campaign was the study of biomass burning, a
30 number of flights were conducted over areas of unperturbed rainforest to study biogenic
31 processes. The flights occurred after the onset of the transition to the wet season, where the

1 weather within Brazil became more unsettled. Due to wet deposition and a change in synoptic
2 transport, this resulted in generally lower concentrations of anthropogenic emissions
3 compared to the later stages of the dry season, when biomass burning was at its peak.

4 In total, 5 biogenic flights took place, which are summarised in Fig. 2 and Table 1. The first
5 flight, B735, partly collected high-altitude data between Porto Velho and Manaus, however
6 periods of flying over the rainforest also took place. The remaining four flights took place out
7 of Porto Velho and followed a similar format to that used during OP3, where one flight took
8 place around midday (local time), with a second flight in the afternoon after refuelling. This
9 was designed such that the chemistry could be contrasted, with the expectation that the
10 midday flight would occur when the biogenic VOCs would be at their peak and the afternoon
11 flight when the oxidation products would be more significant. B744 and B745 took place over
12 the Pacaás Novos national park to the south of Porto Velho in Rondônia and B749 and B750
13 flew over the rainforest in Amazonas to the north of Porto Velho.

14 **2.2 Instrumentation**

15 All of the onboard aerosol instruments used Rosemount inlets (Foltescu et al., 1995). While
16 these are known to incur sampling artefacts for larger particles, they are deemed adequate for
17 submicron particles of interest here (Trembath et al., 2012). Naphion driers were used
18 upstream of the aerosol instruments to prevent condensation of water in the inlet lines (but not
19 to specifically sample the aerosol ‘dry’), meaning aerosols were typically sampled at an RH
20 of around 50-60 %.

21 An Aerodyne Research (Billerica, MA, USA) Aerosol Mass Spectrometer (AMS) was used to
22 make measurements of nonrefractory aerosol composition. This was a Compact Time of
23 Flight (CTOF) type AMS (Canagaratna et al., 2007; Drewnick et al., 2005), as used in OP3
24 and other previous FAAM publications (Robinson et al., 2011; Morgan et al., 2010b).
25 Detection limits are around 40 ng m^{-3} for organics and ammonium and 5 ng m^{-3} for nitrate and
26 sulphate (Drewnick et al., 2009), with an estimated accuracy (neglecting uncertainty in
27 collection efficiency) of around 10 %. Calibrations were performed using monodisperse
28 ammonium nitrate and ammonium sulphate to generate ionisation efficiency data for nitrate
29 and relative ionisation efficiencies for ammonium and sulphate. Equivalent volume
30 concentrations incorporating black carbon data (see below) and using the densities
31 recommended by Cross et al. (2007) were compared against those from a Scanning Mobility

1 Particle Sizer (SMPS) and the comparison was good (85-90 % of SMPS volume) if a
2 collection efficiency (CE) of 1 was used for most flights during the campaign. Certain flights
3 (in particular B749 and B750) had less favourable volume comparisons (around 50 %),
4 however these took place during higher humidity conditions (see below) and given that the
5 SMPS employed no sheath air drying, its data are seen as an unreliable reflection of the ‘dry’
6 volume measured by the AMS under these conditions, so a CE of 1 is assumed for all flights
7 for the sake of internal consistency. This is inconsistent with the parameterisation of
8 Middlebrook et al. (2012), where a lower CE would be expected (based on the inorganic
9 composition not being dominated by either ammonium nitrate or sulphuric acid and the
10 sampling humidity being less than 80 %), but is the same as previous observations in the
11 Amazon presented by Chen et al. (2009), who ascribed the higher CE to the organically-
12 dominated particles adopting a liquid phase. An exception to these was B735, where the AMS
13 reported an equivalent volume concentration of around an order of magnitude less than that of
14 the SMPS. At the time, the inlet flow was reduced, indicating a partial blockage of the inlet
15 pinhole. The pinhole was cleaned afterwards and subsequent data had more favourable
16 comparisons with the SMPS and other instruments, implying the blockage was causing a large
17 fraction of the particles to be lost at the inlet. However, the data are still included here because
18 the data on mass ratios should still be representative of the ambient. This is assuming that the
19 losses apply to all chemical constituents equally; while the losses may be size-dependent, the
20 composition is likely to be equal for all sizes if it is dominated by secondary material.

21 Measurements of black carbon were made using a Droplet Measurement Technologies
22 (Boulder, CO, USA) Single Particle Soot Photometer (SP2). This is the same instrument that
23 was used in previous FAAM publications (McMeeking et al., 2010). It was calibrated using
24 monodisperse AquaDAG (Acheson Industries), with a correction of 0.75 applied according to
25 Laborde et al. (2012a). The instrument measures refractory black carbon, denoted as rBC
26 according to the definitions recommended by Petzold et al. (2013). Note that the SP2 employs
27 active drying on its sheath air system, so particles are sampled at a low RH. Overall accuracy
28 is estimated at around 20 % with 90 nm sphere equivalent rBC volume necessary for particle
29 detection (Laborde et al., 2012b).

30 Measurements of isoprene were made using an on board proton transfer reaction mass
31 spectrometer (PTR-MS, Ionicon, Innsbruck, Austria) containing a quadrupole detector. The
32 instrument measured a range of hydrocarbons and oxygenated hydrocarbons with a typical

1 cycle time of around 3-5 s. Isoprene was calibrated against gas standards provided by Apel-
2 Reimer Environmental (Broomfield, CO, USA). The instrument was the same as used during
3 OP3 and full instrumental, operational and calibration details are described in Murphy et al.
4 (2010). Accuracy for isoprene is estimated at $\pm 15\%$ and data were validated against offline
5 gas chromatography analysis of samples taken using the aircraft's Whole Air Sampling
6 (WAS) system, using the methods described by Hopkins et al. (2011).

7 Measurements of NO were made using a custom built chemiluminescence instrument (Air
8 Quality Design Inc, Wheat Ridge, CO, USA), with NO₂ measured on a second channel after
9 photolytic conversion to NO. The instrument was the same as used during OP3 (Pike et al.,
10 2010) and the use of photolytic (as opposed to catalytic) conversion eliminates possible
11 interference from NO_x on the NO₂ channel. Detection limits are on the order of 10 pptv for
12 NO and 15 pptv for NO₂ for 10 second averaged data, with estimated accuracies of 15% for
13 NO at 0.1 ppbv and 20% for NO₂ at 0.1 ppbv.

14 Navigational data was provided by an Applanix (Richmond Hill, ON, Canada) POS AV 510
15 GPS-aided inertial navigational unit and altitudes are quoted as above mean sea level.
16 Temperature and pressure were provided by flight instrumentation and humidity was
17 measured (as a dew point accurate to ± 0.2 °C) using two chilled mirror hygrometers; a
18 General Eastern 1011B (GE Measurement & Control) and a Buck Research Instruments
19 (Boulder, CO, USA) model CR2. The data presented here is derived from the General Eastern
20 instrument, although the two instruments were in good agreement.

21 **3 Results**

22 **3.1 General results**

23 Because the chemical processes are known to principally take place in the boundary layer, the
24 primary statistics have been calculated for those periods of the flights where the aircraft was
25 below an altitude of 2 km. Take-offs, landings and approaches were excluded from the
26 analysis to eliminate the influences of the airports and associated cities.

27 In addition to the total organic matter (Org_{Total}), the organic contribution from $m/z=82$ is also
28 shown (Org₈₂), with the same relative ionisation efficiency (RIE) applied (1.4). As can be
29 seen, none of the flights were completely free of influence from combustion (assumed
30 anthropogenic) sources, as evidenced by the presence rBC. The concentrations of
31 anthropogenic emissions were highest in B744 and B745, which also featured the highest

1 organic mass concentrations. This may be due to agricultural activities elsewhere in
2 Rondônia. However, the concentrations in general would still be considered lower than the
3 regional polluted hazes (Darbyshire et al., manuscript in preparation for this special issue), so
4 we postulate that pollution levels have been reduced through mixing with cleaner air or wet
5 deposition. Nitrate was also reported in all of the flights, using the standard AMS
6 fragmentation tables (Allan et al., 2004), although as will be shown below, there is reason to
7 suspect this may not entirely be due to ammonium nitrate. Isoprene was present in all the
8 flights, indicating that strong biogenic emissions and associated chemical processes were
9 taking place.

10 Further information regarding the composition of the aerosol and possible chemical processes
11 can be obtained by inspecting correlations and ratios between the various measured quantities.
12 These are shown in Table 2. With the exception of B735 (whose data had a low signal-to-
13 noise ratio), the correlations between Org_{82} and $\text{Org}_{\text{Total}}$ were generally better than those
14 reported by Robinson et al. (2011), which is almost certainly due to the lack of ground-based
15 anthropogenic sources; OP3 was heavily impacted by emissions associated with palm oil
16 agriculture and processing, which provided a large source of variability in organic
17 composition. In contrast, the composition of the organic aerosol was more homogeneous here.
18 The $\text{Org}_{82}/\text{Org}_{\text{Total}}$ ratios for B744 and B745 were consistent with the lower end of the scale
19 presented by Robinson et al. (2011), whereas B735, B749 and B750 were very high in
20 comparison, implying the methylfuran marker was not present in B744 and B745, but present
21 in the others.

22 Using the default data products, all flights would appear to have significant ammonium nitrate
23 concentrations, which would imply that the aerosol was pH neutral, as nitrate would partition
24 into the gas phase as nitric acid in the presence of acidic sulphate particles. However, this is at
25 odds with the comparison between the measured ammonium and the calculated amounts of
26 ammonium that would be required to neutralise the sulphate and nitrate measured
27 ($\text{NH}_4^+/\text{NH}_4^+_{\text{Neut}}$), which implies that B735, B749 and B750 had acidic aerosols. Organic
28 nitrogen species can also contribute to the apparent nitrate signal, a phenomenon that has been
29 reported in other forested environments (Allan et al., 2006). A key diagnostic is the
30 comparison of the signals at m/z 30 and 46 (M_{30} and M_{46}), as organic nitrates and amines will
31 give stronger signals at 30 (as NO^+ and CNH_4^+ respectively) over 46 (NO_2^+), compared to
32 ammonium nitrate. As can be seen in Table 2, all flights reported higher values than the

1 ammonium nitrate ratio of 1.54 measured during calibrations, implying that organic nitrogen
2 was present. It should be noted that a signal at 30 can also arise from CH_2O^+ ions from
3 oxygenated organics. While this generally tends to be a very minor organic fragment under
4 most ambient conditions, the dominance of organics over inorganics in this instance means
5 that it cannot be ruled out. However, this being the case, this would not detract from the
6 argument that it is not as a result of inorganic nitrate.

7 On the assumption that the nitrate reported was not ammonium nitrate, the ammonium
8 balance calculation was repeated for sulphate in isolation ($\text{NH}_4^+/\text{NH}_4^+\text{SO}_4$). According to this,
9 B735, B749 and B750 were still judged acidic, whereas B744 and B745 apparently had an
10 excess of ammonium. This is again not deemed physically possible, as under alkaline
11 conditions, ammonium partitions into the gas phase as ammonia. This, along with the lower
12 M_{30}/M_{46} value, leads us to conclude that the reported nitrate was mostly ammonium nitrate
13 and the aerosol was neutral for these two flights, although there is still evidence for there still
14 being at least some organic nitrogen present. While reassigning a portion of the inorganic
15 nitrate would similarly imply an excess of ammonium, a small charge imbalance could be
16 offset by organic acids, which are not included in the calculation.

17 Because rBC was present in all flights, the possibility that biomass burning (or other
18 combustion sources) was responsible for all the organic matter observed must be discounted.
19 The correlation between rBC and $\text{Org}_{\text{Total}}$ was generally weak but not non-existent. There was
20 not an appreciable signal at $m/z=60$, which is often taken as a marker for biomass burning
21 (e.g. Allan et al., 2010; DeCarlo et al., 2010; Alfarra et al., 2007), although it should be noted
22 that this is known to be diminished in aged plumes (Capes et al., 2008; Cubison et al., 2011).
23 Attempts at using PMF did not resolve any meaningful organic factors that correlated with
24 rBC. While these inferences do not rule out a contribution from combustion, they similarly do
25 not rule out a contribution from isoprene SOA. This issue is discussed further in the following
26 section.

27 **3.2 Vertical structure**

28 One of the runs during B749 was performed using a ‘sawtooth’ manoeuvre, with a sequence
29 of three profile ascents and descents designed to probe the structure of the boundary layer and
30 lower troposphere. The results of this are shown in Fig. 3. Figure 3a shows the organic mass
31 concentration was highest at an altitude of approximately 1.5 km. The mass concentrations

1 decreased uniformly with lower and higher altitudes, with the exception of a layer of reduced
2 concentrations at around 2 km during the final ascent and descent.

3 Figure 3b shows the temperature and humidity data for the profiles. The potential temperature
4 (θ) is flat up to 1 km, indicating that a well-mixed boundary layer exists up to this altitude.
5 Above 1 km, a positive gradient in θ but a negative gradient in equivalent potential
6 temperature (θ_e) is observed, showing that the lower free troposphere is conditionally
7 unstable. A similar structure was noted in Borneo and under these conditions, upward
8 transport of material from the boundary layer can occur through nonprecipitating cumulus
9 (Robinson et al., 2012). The low concentrations recorded at 2 km and discussed above
10 corresponds to an anomalously low θ_e and corresponding relative humidity, indicating that
11 this layer of low mass concentrations was a result of clean, dry air being mixed downwards
12 from the free troposphere rather than being transported upwards from the boundary layer.

13 To investigate the behaviour of the organic and rBC fractions further, profiles from the
14 various flights are compared in Fig. 4. B735 was omitted because of the relatively small
15 amount of profile data collected over the forest. Similarly, B750 was also excluded because
16 this flight was subject to significant precipitation, which caused a loss of particulate through
17 wet deposition and inconsistent concentrations along the flight tracks. B744 and B745 are
18 compared against B749, as the low $\text{Org}_{82}/\text{Org}_{\text{Total}}$ case versus the contrasting high case.

19 In both cases, the concentrations decrease with altitude above 1.5 km. In the B744-5 case, the
20 ratios $\text{Org}_{82}/\text{Org}_{\text{Total}}$ and $\text{Org}_{\text{Total}}/\text{rBC}$ show no trend with altitude, suggesting that the aerosol
21 is relatively uniform in composition if not concentration. In contrast, in B749, both metrics
22 show significant vertical structure. The positive gradient in $\text{Org}_{\text{Total}}/\text{rBC}$ is particularly
23 significant, as this indicates that during this flight, the organics do not originate from the same
24 source as the black carbon. If they had a common source, one would expect a uniform profile
25 of $\text{Org}_{\text{Total}}/\text{rBC}$ within the well-mixed boundary layer, as was seen in B744-5 and the polluted
26 regional hazes studied by Darbyshire et al. (in preparation). The organics peak at around 1
27 km, consistent with the formation of SOA at the top of the boundary layer, superimposed on a
28 background of rBC (and potentially some organics). The absolute values of $\text{Org}_{\text{Total}}/\text{rBC}$ are
29 not high compared to the values of approximately 10 noted in the polluted regional hazes, but
30 it should be noted that if a polluted airmass had been subjected to wet deposition (which,
31 given the synoptic conditions, is likely to have been the case), non-rBC particles would be
32 preferentially removed, being larger and more soluble and therefore more subject to in-cloud

1 scavenging. As such, this could result in a background $\text{Org}_{\text{Total}}/\text{rBC}$ being lower, which is
2 increased back to around 10 through the formation of SOA.

3 The fractional contribution from Org_{82} peaks at around 0.5-1 km in B749, which shows this
4 marker is most significant at the top of the boundary layer. It decreases with altitude, but it is
5 worth noting that it does not fully decrease to the 4 ‰ value of B744-5, which is also the
6 general minimum reported by Robinson et al. (2011). Potential reasons for this decrease are
7 covered in the discussion section.

8 The inorganic profiles are shown in Fig. 5. In both cases, the general loadings show an initial
9 increase in concentration with altitude within the boundary layer, although unlike the organic
10 trend in B749, the concentration of sulphate in particular continues to increase beyond 1 km,
11 up to 1.5 km. If sulphate is compared with rBC (as a proxy for regional haze), a positive trend
12 is noted that continues to high altitudes, which is consistent with sulphate originating from
13 sources outside of the Amazon basin and being transported downwards from the free
14 troposphere, as described by Chen et al. (2009). The behaviour of nitrate is interesting, with
15 the M_{30}/M_{46} diagnostic higher within the boundary layer in both cases, which would be
16 consistent with the formation of organic nitrogen. However, when comparing organic mass
17 concentration with M_{30} (as a proxy for organic nitrogen), the two cases show very different
18 behaviour, with the ratio for B749 being roughly constant up to 1.5 km and showing a marked
19 negative gradient for B744-5, which crosses the value of 25 for B749. While the M_{30} may be
20 due to nitro-aromatics have been associated with biomass burning (Mohr et al., 2013), the
21 vertical trends presented here do not match with the rBC, so it is not thought to be the case
22 here. The structure in B744-5 is probably due to the ammonium nitrate present during these
23 flights, which will peak in concentration at the top of the boundary layer (Morgan et al.,
24 2010a; Morgan et al., 2009) and suppress the ratio through an inorganic NO^+ contribution to
25 M_{30} .

26 **4 Discussion**

27 **4.1 Factors affecting formation**

28 The presence of the Org_{82} marker in flights B735, B749 and B750 and its absence in B744
29 and B745 is consistent with it being due to methylfuran from isoprene SOA via the IEPOX
30 route, being formed in an abundance of isoprene, with the cases where it is present being
31 those with the lower NO_x concentrations and acidic seed aerosols. It is unfortunate that the

1 wet deposition that took place in B750 prevented a direct comparison with B749, which
2 would have allowed the changes in chemistry with time of day to be probed in the same
3 manner as Robinson et al. (2011).

4 Unfortunately, based on observations alone, it is not possible to conclusively say which, if
5 any, factor was singularly responsible for the difference in observations. The presence of NO
6 affects the chemical processes through reactions with peroxy radicals, inhibiting the peroxy-
7 peroxy reactions needed to form IEPOX through the ISOPOOH route (Surratt et al., 2010).
8 While model and laboratory systems are frequently referred to as ‘high NO_x’ and ‘low NO_x’,
9 it is difficult to define a discrete cutoff point between the two chemical regimes due to the
10 inherent complexities associated with other aspects of how NO_x and VOCs interact
11 (Wennberg, 2013). Furthermore, recent work by Jacobs et al. (2014) indicates that it is also
12 possible to form IEPOX from isoprene hydroxynitrates in the ‘high NO_x’ regime. While all
13 average NO concentrations were below the approximate figure of 100 pptv often given for
14 when NO-peroxy reactions become important (pp 330-331, in: Faraday Discussions, 2013),
15 without the use of a detailed chemical model (which would be difficult to constrain with the
16 data here), it is difficult to say definitively here whether or not NO_x concentrations were a
17 significant factor in determining SOA formation. However, it is worth noting that Claeys et
18 al. (2010) found that the isoprene SOA markers in Rondônia were highest during the dry
19 season, corresponding to the highest NO_x concentrations, so in this context, it would seem
20 unlikely.

21 The role of aerosol acidity has long been seen as necessary for uptake (Surratt et al., 2007b;
22 Eddingsaas et al., 2010) and this conclusion was supported by observational data from this
23 region presented by Claeys et al. (2010), although recent laboratory results from Nguyen et al.
24 (2014) show that it is possible to form SOA with the *m/z*=82 marker from IEPOX on a neutral
25 ammonium sulphate seed, providing it is aqueous, as opposed to solid. This occurs through
26 ammonium ions (NH₄⁺) acting to catalyse the uptake in the absence of a proton donor. The
27 conditions during B744 and B745 were drier than B749 and B750, with the respective
28 measured relative humidities in the boundary layer ranging from approximately 45 to 70 %
29 instead of 60 to 80 %. The former humidity range is within the metastable regime for pure
30 ammonium sulphate and according to the work of Song et al. (2013), internally mixed
31 ammonium sulphate and organic particles could effloresce under these conditions. As such, it
32 is possible that the inorganic matter during B749 and B750 existed as a solid or as a non-

1 aqueous organic liquid, which would inhibit the formation through the neutral mechanism of
2 Nguyen et al. (2014). Note that the acidic mechanism explored by Surratt et al. (2007b) was
3 shown to be effective at 30 % RH, so it could be inferred that had the aerosol in B744 and
4 B745 been acidic, formation would have taken place, regardless of humidity. Likewise, it
5 could also be inferred that if B749 and B750 had been less humid, formation could have still
6 taken place, due to the aerosols' acidity.

7 While there is considerable interest in the literature concerning the role of sulphur and
8 nitrogen in the formation mechanisms (Nguyen et al., 2014; Gomez-Gonzalez et al., 2008;
9 Surratt et al., 2007a), it should be noted that only very limited conclusions can be drawn here.
10 In addition to the M_{30}/M_{46} data possibly indicating some role of organic nitrogen, the sulphate
11 to rBC ratio shows a positive gradient with altitude within the boundary layer in B749 (albeit
12 a weaker gradient than the equivalent organic ratio). This may point to the measurement being
13 influenced by organosulphates, although the fact that the sulphate ratio continues to increase
14 at a similar rate above 1 km (unlike the organic ratio) would detract from this argument.
15 Ultimately, while these data give some intriguing results, given the difficulties in
16 discriminating and quantifying organic sulphur and nitrogen species with the AMS (in
17 particular with the C-TOF), it is difficult to see that any strong conclusions can be drawn here.
18 Further investigation will require the use of additional measurement techniques.

19 **4.2 Boundary layer profile**

20 B749 provides the best case study when the marker is present and its vertical structure
21 provides many features of interest. The positive gradient through the boundary layer
22 (featuring a doubling of Org_{82} from 20 to 40 ng m^{-3}) could be as a result of the repartitioning
23 of semivolatile material into the aqueous phase due to the reduced temperature and increased
24 particulate water content (Morgan et al., 2010a). This would be consistent with the
25 observations of Fu et al. (2010), who found an increase in isoprene SOA tracers at night-time
26 at an elevated site in China, and the modelling work of Henze and Seinfeld (2006), who
27 predict enhanced partitioning to the particle phase at higher altitudes. To explore the
28 feasibility of this hypothesis, estimates of particulate mass concentrations were made using
29 the PartProp component of the UManSysProp tools
30 (<http://umansysprop.seaes.manchester.ac.uk>), which predicts equilibrium concentrations
31 according to a Gibbs free energy minimisation, allowing for the organic and water contents to
32 be calculated in tandem (e.g. Topping et al., 2013). The methods of organic vapour pressure

1 and boiling point estimation according to Nannoolal et al. (2008; 2004) and non-ideality
2 (including solute-solute interactions) according to AIOMFAC (Zuend et al., 2011; Zuend et
3 al., 2008) were used. A nominal $0.005 \text{ nmol m}^{-3}$ ammonium sulphate seed was assumed
4 (currently, UManSysProp does not allow for inorganic charge imbalance) and particulate
5 organic mass concentrations were compared between conditions typical of the top of the
6 boundary layer (295 K, 80 % RH) and the lowest altitude sampled (302 K, 60% RH). While it
7 will never be possible to fully constrain this model with the data available, it should give an
8 indication of how realistic these hypotheses are. Note for the purposes of this model, all gas
9 phase concentrations are given in molecules per cm^3 .

10 If one assumes that the dominant component of the particle phase giving rise to the
11 methylfuran marker are the 3-MeTHF-3,4-diols, it is found that an unrealistically large
12 concentration of 10^{13} cm^{-3} (corresponding to hundreds of ppb) is needed to predict a mass
13 concentration of 45 ng m^{-3} at the top of the boundary layer, implying that this is not the
14 specific form that is physically present in the particle phase. Given that Lin et al. (2012)
15 reported it as present in ambient particulates (through offline analysis by GC-MS after
16 methanol extraction and trimethylsilylation), it is possible that this exists in the particle phase
17 through a chemical uptake process that is reversed during the analytical process. If a dimer of
18 this molecule is considered, it is found that a concentration of 10^{10} cm^{-3} gives a mass
19 concentration of between 35 and 102 ng m^{-3} at the top of the boundary layer, depending on
20 the isomer (higher mass concentrations are favoured when both methyl groups are adjacent to
21 the ether group). When these concentrations are compared with the conditions at the bottom
22 of the boundary layer, concentrations between 22 and 55 ng m^{-3} are predicted, which
23 correspond to a reduction in mass of 37 to 46 %. Repeating the calculation for 2-methyltetrol,
24 the concentration at the top of the boundary layer is predicted as $2.08 \text{ } \mu\text{g m}^{-3}$, compared to
25 $1.27 \text{ } \mu\text{g m}^{-3}$ at the bottom, a reduction of 39 %. While this model carries an inherent
26 uncertainty and the actual particulates are likely to be formed of a complex mixture of many
27 species, these estimates show that repartitioning could conceivably be responsible for the
28 observed change in mass with altitude, although it is recognised that if higher order oligomers
29 are the dominant form of SOA mass, these are likely to be less volatile and therefore less
30 likely to exhibit this behaviour. For example, when the calculation is repeated for 10^{10} cm^{-3} of
31 a 2-methyltetrol dimer, a concentration of $4.22 \text{ } \mu\text{g m}^{-3}$ is predicted for both altitudes.

1 An alternative hypothesis is that the peak at the top of the boundary layer reflects faster
2 production rate of SOA at this altitude. The aerosol concentrations were not sufficient to
3 affect actinic flux within the boundary layer (as evidenced by the aircraft's pyranometer
4 measurements during the profiles), so it is assumed that gas-phase photochemistry was not
5 promoted significantly at the top of the boundary layer. It should be noted that Karl et al.
6 (2007) found evidence of enhanced isoprene photochemistry above the Amazon at cloud level
7 that was attributed to scattered light from cumulous clouds. While this may be possible here, a
8 similar analysis of MVK+MACR relative to isoprene did not show the pronounced
9 enhancement at cloud level noted in that paper. Hypothetically, it is possible that the reduced
10 temperature at altitude may also be affecting the chemical reactions, but this is difficult to test
11 here without detailed modelling that is difficult to constrain.

12 Instead, it could be that production is promoted by an increased rate of IEPOX uptake. Using
13 the same model conditions described above for the 3-MeTHF-3,4-diol dimer case, but with
14 10^{10} cm^{-3} of β -IEPOX also included, it is predicted that the equilibrium aqueous
15 concentrations of IEPOX will increase by only 3.6 % at the top of the boundary layer (272 to
16 282 ppm with respect to water). Given this, it would not seem that an increase in
17 concentration due to equilibrium partitioning could be responsible for an increased production
18 rate. Another possible reason for an enhanced production rate could be if the process is
19 kinetically limited by the particulate surface area, which will increase in line with the water
20 content of the particles. However, given the high proportion of organic to inorganic material
21 in the particles (see Table 1), the amount of geometric growth between 60 and 80 % is likely
22 to be small (Gysel et al., 2004); using the HygroProp tool on the 3-MeTHF-3,4-diol dimer
23 case and invoking the density estimation method of Girolami (1994), an increase of only 5.6
24 % in particle surface area between the two altitudes is predicted, so this again does not seem
25 likely.

26 Another hypothesis could be that the particles are undergoing phase changes with altitude,
27 which could affect both the partitioning and the production rate of the SOA. As well as the
28 phase effect on inorganic ion chemistry discussed described by Nguyen et al. (2014), the
29 organic fraction is known to potentially exhibit exotic behaviours such as forming amorphous
30 states and separations from the aqueous phase (Virtanen et al., 2010; Song et al., 2013), which
31 may affect how the particles interact with the gas phase. This is a difficult concept to test with
32 the data available, as there are no measurement data on the hygroscopicity of the particles or

1 the exact phase of the organic fraction. However, the humidity during B749 is significantly
2 higher than the B744-5 case and given that the boundary layer is well-mixed (providing a
3 means for metastable particles to encounter higher humidities), it would seem reasonable to
4 expect all the particles to be aqueous during B749. Phase is also known to affect the CE of the
5 AMS (Matthew et al., 2008), so it is conceptually possible that rather than altering ambient
6 composition, phase changes are creating an artefact within the AMS. Because the SMPS data
7 is regarded as unreliable during profiles (due to the continuous pressure change affecting
8 flows), a comparison of the AMS-derived volume concentration was compared against an
9 equivalent derived from the SP2 scattering data (calibrated using polystyrene latex spheres).
10 While this method has uncertainties associated with ambiguities in the optical properties of
11 ambient particles, the comparison showed no trend with altitude, implying that there was no
12 change in CE.

13 A final, somewhat speculative, hypothesis is that the gradient exists because of a loss
14 mechanism at the bottom of the boundary layer, in turn causing a gradient to exist within the
15 well-mixed layer. If one assumes that sulphate is all from out-of-basin sources, this would
16 seem a reasonable explanation because this too exhibits a positive gradient with altitude
17 within the boundary layer during B749. While it is generally assumed that dry deposition is
18 not significant for involatile submicron particles, it is possible that during interactions with
19 the forest canopy (Whitehead et al., 2010), the aerosols are exposed to much higher
20 humidities and undergo growth or even activation, followed by loss by impaction. This would
21 not be inconsistent with the lack of a vertical trend in rBC, as these are smaller and less
22 hygroscopic and therefore would be less affected by this process. Given that there are no in-
23 canopy data available here, this hypothesis is impossible to test.

24 **4.3 Free tropospheric profile**

25 The behaviour above the boundary layer is also of interest. The overall concentrations
26 decrease with altitude as material from the boundary layer is mixed with cleaner and drier free
27 tropospheric air. There is also a shift in composition in terms of $\text{Org}_{82}/\text{Org}_{\text{Total}}$ with altitude.
28 This could be due to mixing with a background of organic matter from a different source
29 (natural or anthropogenic), but if it can be assumed that the material at higher altitudes
30 originally resembled that within the boundary layer, this would offer an insight to the fate of
31 these aerosols.

1 Figure 6a shows the numerical difference in the normalised mass spectra of organic mass
2 between the boundary layer and the lower free troposphere. The comparison shows a general
3 transition between mass spectra that resembles the evolution from semivolatile (SV) to low
4 volatility (LV) oxygenated organic aerosol (OOA) described by Jimenez et al. (2009), albeit
5 with the presence of the methylfuran marker in the SV-OOA equivalent spectrum. Note that
6 this is not to say that the boundary layer state is necessarily semivolatile, but may represent a
7 less chemically aged version of that which is transported higher into the troposphere. This
8 general trend is further reinforced by Fig. 6b, which shows the $\text{Org}_{44}/\text{Org}_{\text{Total}}$ (often referred to
9 as ' f_{44} ' elsewhere in the literature) during B749 reaches a minimum at approximately 1 km
10 (the peak in $\text{Org}_{82}/\text{Org}_{\text{Total}}$), with a value of 0.12, before increasing steadily through to a value
11 of 0.16 at 3km. Conversely, B744-5 shows a general increase throughout the altitude range.

12 As it is transported upwards, the organic matter will be subject to oxidation processes (that
13 may include aqueous processing during wet convection), which will add oxygenated
14 functionality (McFiggans et al., 2005; Kroll et al., 2011). As the chemical ageing progresses,
15 the mass spectral profile begins to resemble that of LV-OOA, which is dominated by CO_2^+
16 from the thermal decomposition of multifunctional species. While this change in profile could
17 be the result of the addition of new, more oxidised SOA on top of the existing material, this is
18 not deemed likely because the $\text{Org}_{\text{Total}}/\text{rBC}$ ratio, if anything, decreases with altitude above
19 the boundary layer, according to Fig. 4. All this being the case, this has important
20 implications for the usage of methylfuran as an isoprene SOA marker, as it indicates that it is
21 not conserved within the atmosphere and is therefore only useful as a marker in the near field.

22 **5 Conclusions**

23 Presented here are AMS observations of organic matter measured above the Amazon
24 rainforest, taken over five flights as part of the SAMBBA campaign on the FAAM BAe-146
25 research aircraft. Through the investigation of the previously-identified marker at $m/z=82$
26 (corresponding to methylfuran), it is suggested that isoprene SOA is being formed within the
27 boundary layer under certain conditions. A comparison between flights where the marker is
28 found with those where it was not indicate behaviour consistent with formation through the
29 IEPOX route, with the marker's presence favouring the flights with low NO_x concentrations,
30 acidic seed particles and higher relative humidity. In addition, data suggests a role of organic
31 nitrogen in the chemistry. It should be noted that the rBC and NO_x concentrations were

1 consistently low but exhibited some residual pollution, indicating that conditions do not have
2 to be pristine for this mechanism to take place, in agreement with Claeys et al. (2010).

3 A specific flight (B749) provided the best case study for this process and an inspection of
4 vertical profiles yielded some interesting behaviour in the organic mass concentrations and
5 the $m/z=82$ marker. Profiles within the boundary layer show that concentrations are greatest at
6 the top of the boundary layer, with thermodynamic calculations showing that semivolatile
7 repartitioning of SOA is a plausible explanation, in line with Henze and Seinfeld (2006). The
8 behaviour of the marker within the free troposphere suggests that through atmospheric
9 processing, the mass spectral profile changes to that of the highly processed organic matter
10 seen in many other environments. While this could be due to mixing with a highly-processed
11 free tropospheric background aerosol, it is also consistent with progressive oxidation and
12 functionalization of the organic matter. If this is the case, it implies that the $m/z=82$ marker is
13 not conserved and therefore may only be suitable as a marker in the near-field. More work in
14 the laboratory and comparisons with other observations in the field are needed to investigate
15 these hypotheses further.

16 **Data availability**

17 Processed data is available at the British Atmospheric Data Centre SAMBBA archive
18 (http://badc.nerc.ac.uk/cgi-bin/data_browser/data_browser/badc/sambba/data/). Raw data are
19 archived at the University of Manchester and available on request.

20 **Acknowledgements**

21 This work was supported by the UK Natural Environment Research Council [NERC] through
22 the SAMBBA project [grant ref: NE/J010073/1] and a PhD studentship [Eoghan Darbyshire].
23 Airborne data was obtained using the BAe-146-301 Atmospheric Research Aircraft [ARA]
24 flown by Directflight Ltd and managed by the Facility for Airborne Atmospheric
25 Measurements [FAAM], which is a joint entity of NERC and the Met Office. We thank Ben
26 Johnson [Met Office] and Karla M. Longo [National Institute for Space Research (INPE),
27 Brazil] for their roles in coordinating the campaign. Isoprene data from WAS sample analysis
28 was provided by James R. Hopkins [National Centre for Atmospheric Science & University
29 of York]. Additional thanks are given to David O. Topping [National Centre for Atmospheric
30 Science & University of Manchester] for the helpful discussions and assistance in the use of
31 the UManSysProp tools.

1 **References**

- 2 Alfarra, M. R., Prevot, A. S. H., Szidat, S., Sandradewi, J., Weimer, S., Lanz, V. A.,
3 Schreiber, D., Mohr, M., and Baltensperger, U.: Identification of the mass spectral signature
4 of organic aerosols from wood burning emissions, *Environ. Sci. Technol.*, 41, 5770-5777, Doi
5 10.1021/Es062289b, 2007.
- 6 Allan, J. D., Delia, A. E., Coe, H., Bower, K. N., Alfarra, M. R., Jimenez, J. L., Middlebrook,
7 A. M., Drewnick, F., Onasch, T. B., Canagaratna, M. R., Jayne, J. T., and Worsnop, D. R.: A
8 generalised method for the extraction of chemically resolved mass spectra from aerodyne
9 aerosol mass spectrometer data, *J. Aerosol. Sci.*, 35, 909-922, DOI
10 10.1016/j.jaerosci.2004.02.007, 2004.
- 11 Allan, J. D., Alfarra, M. R., Bower, K. N., Coe, H., Jayne, J. T., Worsnop, D. R., Aalto, P. P.,
12 Kulmala, M., Hyotylainen, T., Cavalli, F., and Laaksonen, A.: Size and composition
13 measurements of background aerosol and new particle growth in a Finnish forest during
14 QUEST 2 using an Aerodyne Aerosol Mass Spectrometer, *Atmos. Chem. Phys.*, 6, 315-327,
15 2006.
- 16 Allan, J. D., Williams, P. I., Morgan, W. T., Martin, C. L., Flynn, M. J., Lee, J., Nemitz, E.,
17 Phillips, G. J., Gallagher, M. W., and Coe, H.: Contributions from transport, solid fuel
18 burning and cooking to primary organic aerosols in two UK cities, *Atmos. Chem. Phys.*, 10,
19 647-668, 2010.
- 20 Budisulistiorini, S. H., Canagaratna, M. R., Croteau, P. L., Marth, W. J., Baumann, K.,
21 Edgerton, E. S., Shaw, S. L., Knipping, E. M., Worsnop, D. R., Jayne, J. T., Gold, A., and
22 Surratt, J. D.: Real-Time Continuous Characterization of Secondary Organic Aerosol Derived
23 from Isoprene Epoxydiols in Downtown Atlanta, Georgia, Using the Aerodyne Aerosol
24 Chemical Speciation Monitor, *Environ. Sci. Technol.*, 47, 5686-5694, 10.1021/es400023n,
25 2013.
- 26 Canagaratna, M. R., Jayne, J. T., Jimenez, J. L., Allan, J. D., Alfarra, M. R., Zhang, Q.,
27 Onasch, T. B., Drewnick, F., Coe, H., Middlebrook, A., Delia, A., Williams, L. R., Trimborn,
28 A. M., Northway, M. J., DeCarlo, P. F., Kolb, C. E., Davidovits, P., and Worsnop, D. R.:
29 Chemical and microphysical characterization of ambient aerosols with the aerodyne aerosol
30 mass spectrometer, *Mass Spectrom. Rev.*, 26, 185-222, Doi 10.1002/Mas.20115, 2007.

1 Capes, G., Johnson, B., McFiggans, G., Williams, P. I., Haywood, J., and Coe, H.: Aging of
2 biomass burning aerosols over West Africa: Aircraft measurements of chemical composition,
3 microphysical properties, and emission ratios, *J. Geophys. Res.-Atmos.*, 113, D00c15, Doi
4 10.1029/2008jd009845, 2008.

5 Carlton, A. G., Wiedinmyer, C., and Kroll, J. H.: A review of Secondary Organic Aerosol
6 (SOA) formation from isoprene, *Atmos. Chem. Phys.*, 9, 4987-5005, 10.5194/acp-9-4987-
7 2009, 2009.

8 Chan, M. N., Surratt, J. D., Claeys, M., Edgerton, E. S., Tanner, R. L., Shaw, S. L., Zheng,
9 M., Knipping, E. M., Eddingsaas, N. C., Wennberg, P. O., and Seinfeld, J. H.:
10 Characterization and Quantification of Isoprene-Derived Epoxydiols in Ambient Aerosol in
11 the Southeastern United States, *Environ. Sci. Technol.*, 44, 4590-4596, Doi
12 10.1021/Es100596b, 2010.

13 Chen, Q., Farmer, D. K., Schneider, J., Zorn, S. R., Heald, C. L., Karl, T. G., Guenther, A.,
14 Allan, J. D., Robinson, N., Coe, H., Kimmel, J. R., Pauliquevis, T., Borrmann, S., Poschl, U.,
15 Andreae, M. O., Artaxo, P., Jimenez, J. L., and Martin, S. T.: Mass spectral characterization
16 of submicron biogenic organic particles in the Amazon Basin, *Geophys. Res. Lett.*, 36,
17 L20806, 10.1029/2009gl039880, 2009.

18 Chen, Q., Farmer, D. K., Rizzo, L. V., Pauliquevis, T., Kuwata, M., Karl, T. G., Guenther, A.,
19 Allan, J. D., Coe, H., Andreae, M. O., Pöschl, U., Jimenez, J. L., Artaxo, P., and Martin, S. T.:
20 Fine-mode organic mass concentrations and sources in the Amazonian wet season (AMAZE-
21 08), *Atmos. Chem. Phys. Discuss.*, 14, 16151-16186, 10.5194/acpd-14-16151-2014, 2014.

22 Claeys, M., Graham, B., Vas, G., Wang, W., Vermeylen, R., Pashynska, V., Cafmeyer, J.,
23 Guyon, P., Andreae, M. O., Artaxo, P., and Maenhaut, W.: Formation of secondary organic
24 aerosols through photooxidation of isoprene, *Science*, 303, 1173-1176, DOI
25 10.1126/science.1092805, 2004.

26 Claeys, M., Kourtchev, I., Pashynska, V., Vas, G., Vermeylen, R., Wang, W., Cafmeyer, J.,
27 Chi, X., Artaxo, P., Andreae, M. O., and Maenhaut, W.: Polar organic marker compounds in
28 atmospheric aerosols during the LBA-SMOCC 2002 biomass burning experiment in
29 Rondônia, Brazil: sources and source processes, time series, diel variations and size
30 distributions, *Atmos. Chem. Phys.*, 10, 9319-9331, 10.5194/acp-10-9319-2010, 2010.

1 Cross, E. S., Slowik, J. G., Davidovits, P., Allan, J. D., Worsnop, D. R., Jayne, J. T., Lewis,
2 D. K., Canagaratna, M., and Onasch, T. B.: Laboratory and ambient particle density
3 determinations using light scattering in conjunction with aerosol mass spectrometry, *Aerosol*
4 *Sci. Technol.*, 41, 343-359, Doi 10.1080/02786820701199736, 2007.

5 Cubison, M. J., Ortega, A. M., Hayes, P. L., Farmer, D. K., Day, D., Lechner, M. J., Brune,
6 W. H., Apel, E., Diskin, G. S., Fisher, J. A., Fuelberg, H. E., Hecobian, A., Knapp, D. J.,
7 Mikoviny, T., Riemer, D., Sachse, G. W., Sessions, W., Weber, R. J., Weinheimer, A. J.,
8 Wisthaler, A., and Jimenez, J. L.: Effects of aging on organic aerosol from open biomass
9 burning smoke in aircraft and laboratory studies, *Atmos. Chem. Phys.*, 11, 12049-12064, DOI
10 10.5194/acp-11-12049-2011, 2011.

11 Czoschke, N. M., Jang, M., and Kamens, R. M.: Effect of acidic seed on biogenic secondary
12 organic aerosol growth, *Atmos. Environ.*, 37, 4287-4299, 2003.

13 DeCarlo, P. F., Ulbrich, I. M., Crouse, J., de Foy, B., Dunlea, E. J., Aiken, A. C., Knapp, D.,
14 Weinheimer, A. J., Campos, T., Wennberg, P. O., and Jimenez, J. L.: Investigation of the
15 sources and processing of organic aerosol over the Central Mexican Plateau from aircraft
16 measurements during MILAGRO, *Atmos. Chem. Phys.*, 10, 5257-5280, 10.5194/acp-10-
17 5257-2010, 2010.

18 Drewnick, F., Hings, S. S., DeCarlo, P., Jayne, J. T., Gonin, M., Fuhrer, K., Weimer, S.,
19 Jimenez, J. L., Demerjian, K. L., Borrmann, S., and Worsnop, D. R.: A New Time-of-Flight
20 Aerosol Mass Spectrometer (TOF-AMS)-Instrument Description and First Field Deployment,
21 *Aerosol Sci. Technol.*, 39, 637-658, 2005.

22 Drewnick, F., Hings, S. S., Alfarra, M. R., Prevot, A. S. H., and Borrmann, S.: Aerosol
23 quantification with the Aerodyne Aerosol Mass Spectrometer: detection limits and ionizer
24 background effects, *Atmos. Meas. Tech.*, 2, 33-46, 2009.

25 Eddingsaas, N. C., VanderVelde, D. G., and Wennberg, P. O.: Kinetics and Products of the
26 Acid-Catalyzed Ring-Opening of Atmospherically Relevant Butyl Epoxy Alcohols, *The*
27 *Journal of Physical Chemistry A*, 114, 8106-8113, 10.1021/jp103907c, 2010.

28 Faraday Discussions: General discussion, *Faraday Discuss.*, 165, 317-342, doi:
29 10.1039/C3FD90033A, 2013.

1 Foltescu, V. L., Selin, E., and Below, M.: Corrections for Particle Losses and Sizing Errors
2 during Aircraft Aerosol Sampling Using a Rosemount Inlet and the Pms Las-X, *Atmos.*
3 *Environ.*, 29, 449-453, 1995.

4 Fu, P. Q., Kawamura, K., Kanaya, Y., and Wang, Z. F.: Contributions of biogenic volatile
5 organic compounds to the formation of secondary organic aerosols over Mt Tai, Central East
6 China, *Atmos. Environ.*, 44, 4817-4826, DOI 10.1016/j.atmosenv.2010.08.040, 2010.

7 Girolami, G. S.: A Simple Back of the Envelope Method for Estimating the Densities and
8 Molecular Volumes of Liquids and Solids, *J Chem Educ*, 71, 962-964, 1994.

9 Gomez-Gonzalez, Y., Surratt, J. D., Cuyckens, F., Szmigielski, R., Vermeylen, R., Jaoui, M.,
10 Lewandowski, M., Offenberg, J. H., Kleindienst, T. E., Edney, E. O., Blockhuys, F., Van
11 Alsenoy, C., Maenhaut, W., and Claeys, M.: Characterization of organosulfates from the
12 photooxidation of isoprene and unsaturated fatty acids in ambient aerosol using liquid
13 chromatography/(-) electrospray ionization mass spectrometry, *J Mass Spectrom*, 43, 371-
14 382, Doi 10.1002/Jms.1329, 2008.

15 Guenther, A., Karl, T., Harley, P., Wiedinmyer, C., Palmer, P. I., and Geron, C.: Estimates of
16 global terrestrial isoprene emissions using MEGAN (Model of Emissions of Gases and
17 Aerosols from Nature), *Atmos. Chem. Phys.*, 6, 3181-3210, 10.5194/acp-6-3181-2006, 2006.

18 Gysel, M., Weingartner, E., Nyeki, S., Paulsen, D., Baltensperger, U., Galambos, I., and Kiss,
19 G.: Hygroscopic properties of water-soluble matter and humic-like organics in atmospheric
20 fine aerosol, *Atmos. Chem. Phys.*, 4, 35-50, 2004.

21 Hallquist, M., Wenger, J. C., Baltensperger, U., Rudich, Y., Simpson, D., Claeys, M.,
22 Dommen, J., Donahue, N. M., George, C., Goldstein, A. H., Hamilton, J. F., Herrmann, H.,
23 Hoffmann, T., Iinuma, Y., Jang, M., Jenkin, M. E., Jimenez, J. L., Kiendler-Scharr, A.,
24 Maenhaut, W., McFiggans, G., Mentel, T. F., Monod, A., Prevot, A. S. H., Seinfeld, J. H.,
25 Surratt, J. D., Szmigielski, R., and Wildt, J.: The formation, properties and impact of
26 secondary organic aerosol: current and emerging issues, *Atmos. Chem. Phys.*, 9, 5155-5236,
27 2009.

28 Henze, D. K., and Seinfeld, J. H.: Global secondary organic aerosol from isoprene oxidation,
29 *Geophys. Res. Lett.*, 33, L09812, 10.1029/2006GL025976, 2006.

30 Hewitt, C. N., Lee, J. D., MacKenzie, A. R., Barkley, M. P., Carslaw, N., Carver, G. D.,
31 Chappell, N. A., Coe, H., Collier, C., Commane, R., Davies, F., Davison, B., Di Carlo, P., Di

1 Marco, C. F., Dorsey, J. R., Edwards, P. M., Evans, M. J., Fowler, D., Furneaux, K. L.,
2 Gallagher, M., Guenther, A., Heard, D. E., Helfter, C., Hopkins, J., Ingham, T., Irwin, M.,
3 Jones, C., Karunaharan, A., Langford, B., Lewis, A. C., Lim, S. F., MacDonald, S. M.,
4 Mahajan, A. S., Malpass, S., McFiggans, G., Mills, G., Misztal, P., Moller, S., Monks, P. S.,
5 Nemitz, E., Nicolas-Perea, V., Oetjen, H., Oram, D. E., Palmer, P. I., Phillips, G. J., Pike, R.,
6 Plane, J. M. C., Pugh, T., Pyle, J. A., Reeves, C. E., Robinson, N. H., Stewart, D., Stone, D.,
7 Whalley, L. K., and Yin, X.: Overview: oxidant and particle photochemical processes above a
8 south-east Asian tropical rainforest (the OP3 project): introduction, rationale, location
9 characteristics and tools, *Atmos. Chem. Phys.*, 10, 169-199, 10.5194/acp-10-169-2010, 2010.

10 Hopkins, J. R., Jones, C. E., and Lewis, A. C.: A dual channel gas chromatograph for
11 atmospheric analysis of volatile organic compounds including oxygenated and monoterpene
12 compounds, *J Environ Monitor*, 13, 2268-2276, 10.1039/C1EM10050E, 2011.

13 Jacobs, M. I., Burke, W. J., and Elrod, M. J.: Kinetics of the reactions of isoprene-derived
14 hydroxynitrates: gas phase epoxide formation and solution phase hydrolysis, *Atmos. Chem.*
15 *Phys.*, 14, 8933-8946, 10.5194/acp-14-8933-2014, 2014.

16 Jimenez, J. L., Canagaratna, M. R., Donahue, N. M., Prevot, A. S. H., Zhang, Q., Kroll, J. H.,
17 DeCarlo, P. F., Allan, J. D., Coe, H., Ng, N. L., Aiken, A. C., Docherty, K. S., Ulbrich, I. M.,
18 Grieshop, A. P., Robinson, A. L., Duplissy, J., Smith, J. D., Wilson, K. R., Lanz, V. A.,
19 Hueglin, C., Sun, Y. L., Tian, J., Laaksonen, A., Raatikainen, T., Rautiainen, J., Vaattovaara,
20 P., Ehn, M., Kulmala, M., Tomlinson, J. M., Collins, D. R., Cubison, M. J., E, Dunlea, J.,
21 Huffman, J. A., Onasch, T. B., Alfarra, M. R., Williams, P. I., Bower, K., Kondo, Y.,
22 Schneider, J., Drewnick, F., Borrmann, S., Weimer, S., Demerjian, K., Salcedo, D., Cottrell,
23 L., Griffin, R., Takami, A., Miyoshi, T., Hatakeyama, S., Shimono, A., Sun, J. Y., Zhang, Y.
24 M., Dzepina, K., Kimmel, J. R., Sueper, D., Jayne, J. T., Herndon, S. C., Trimborn, A. M.,
25 Williams, L. R., Wood, E. C., Middlebrook, A. M., Kolb, C. E., Baltensperger, U., and
26 Worsnop, D. R.: Evolution of Organic Aerosols in the Atmosphere, *Science*, 326, 1525-1529,
27 10.1126/science.1180353, 2009.

28 Karl, T., Guenther, A., Yokelson, R. J., Greenberg, J., Potosnak, M., Blake, D. R., and
29 Artaxo, P.: The tropical forest and fire emissions experiment: Emission, chemistry, and
30 transport of biogenic volatile organic compounds in the lower atmosphere over Amazonia, *J.*
31 *Geophys. Res.-Atmos.*, 112, Artn D18302, Doi 10.1029/2007jd008539, 2007.

1 Kiendler-Scharr, A., Andres, S., Bachner, M., Behnke, K., Broch, S., Hofzumahaus, A.,
2 Holland, F., Kleist, E., Mentel, T. F., Rubach, F., Springer, M., Steitz, B., Tillmann, R.,
3 Wahner, A., Schnitzler, J. P., and Wildt, J.: Isoprene in poplar emissions: effects on new
4 particle formation and OH concentrations, *Atmos. Chem. Phys.*, 12, 1021-1030, DOI
5 10.5194/acp-12-1021-2012, 2012.

6 Kroll, J., Ng, N., Murphy, S., Flagan, R., and Seinfeld, J.: Secondary organic aerosol
7 formation from isoprene photooxidation, *Environ. Sci. Technol.*, 40, 1869-1877,
8 10.1021/es0524301, 2006.

9 Kroll, J. H., Donahue, N. M., Jimenez, J. L., Kessler, S. H., Canagaratna, M. R., Wilson, K.
10 R., Altieri, K. E., Mazzoleni, L. R., Wozniak, A. S., Bluhm, H., Mysak, E. R., Smith, J. D.,
11 Kolb, C. E., and Worsnop, D. R.: Carbon oxidation state as a metric for describing the
12 chemistry of atmospheric organic aerosol, *Nature Chemistry*, 3, 133-139, 10.1038/nchem.948,
13 2011.

14 Laborde, M., Mertes, P., Zieger, P., Dommen, J., Baltensperger, U., and Gysel, M.:
15 Sensitivity of the Single Particle Soot Photometer to different black carbon types, *Atmos.*
16 *Meas. Tech.*, 5, 1031-1043, 10.5194/amt-5-1031-2012, 2012a.

17 Laborde, M., Schnaiter, M., Linke, C., Saathoff, H., Naumann, K. H., Möhler, O., Berlenz, S.,
18 Wagner, U., Taylor, J. W., Liu, D., Flynn, M., Allan, J. D., Coe, H., Heimerl, K., Dahlkötter,
19 F., Weinzierl, B., Wollny, A. G., Zannata, M., Cozic, J., Laj, P., Hitzenberger, R., Schwarz, J.
20 P., and Gysel, M.: Single Particle Soot Photometer intercomparison at the AIDA chamber,
21 *Atmos. Meas. Tech.*, 5, 3077-3097, 10.5194/amt-5-3077-2012, 2012b.

22 Lin, Y. H., Zhang, Z. F., Docherty, K. S., Zhang, H. F., Budisulistiorini, S. H., Rubitschun, C.
23 L., Shaw, S. L., Knipping, E. M., Edgerton, E. S., Kleindienst, T. E., Gold, A., and Surratt, J.
24 D.: Isoprene Epoxydiols as Precursors to Secondary Organic Aerosol Formation: Acid-
25 Catalyzed Reactive Uptake Studies with Authentic Compounds, *Environ. Sci. Technol.*, 46,
26 250-258, Doi 10.1021/Es202554c, 2012.

27 Matthew, B. M., Middlebrook, A. M., and Onasch, T. B.: Collection efficiencies in an
28 Aerodyne Aerosol Mass Spectrometer as a function of particle phase for laboratory generated
29 aerosols, *Aerosol Sci. Technol.*, 42, 884-898, 2008.

30 McFiggans, G., Alfarra, M. R., Allan, J., Bower, K., Coe, H., Cubison, M., Topping, D.,
31 Williams, P., Decesari, S., Facchini, C., and Fuzzi, S.: Simplification of the representation of

1 the organic component of atmospheric particulates, *Faraday Discuss.*, 130, 341-362, Doi
2 10.1039/B419435g, 2005.

3 McMeeking, G. R., Hamburger, T., Liu, D., Flynn, M., Morgan, W. T., Northway, M.,
4 Highwood, E. J., Krejci, R., Allan, J. D., Minikin, A., and Coe, H.: Black carbon
5 measurements in the boundary layer over western and northern Europe, *Atmos. Chem. Phys.*,
6 10, 9393-9414, DOI 10.5194/acp-10-9393-2010, 2010.

7 Middlebrook, A. M., Bahreini, R., Jimenez, J. L., and Canagaratna, M. R.: Evaluation of
8 Composition-Dependent Collection Efficiencies for the Aerodyne Aerosol Mass Spectrometer
9 using Field Data, *Aerosol Sci. Technol.*, 46, 258-271, Doi 10.1080/02786826.2011.620041,
10 2012.

11 Mohr, C., Lopez-Hilfiker, F. D., Zotter, P., Prevot, A. S. H., Xu, L., Ng, N. L., Herndon, S.
12 C., Williams, L. R., Franklin, J. P., Zahniser, M. S., Worsnop, D. R., Knighton, W. B., Aiken,
13 A. C., Gorkowski, K. J., Dubey, M. K., Allan, J. D., and Thornton, J. A.: Contribution of
14 Nitrated Phenols to Wood Burning Brown Carbon Light Absorption in Detling, United
15 Kingdom during Winter Time, *Environ. Sci. Technol.*, 47, 6316-6324, Doi
16 10.1021/Es400683v, 2013.

17 Morgan, W. T., Allan, J. D., Bower, K. N., Capes, G., Crosier, J., Williams, P. I., and Coe, H.:
18 Vertical distribution of sub-micron aerosol chemical composition from North-Western Europe
19 and the North-East Atlantic, *Atmos. Chem. Phys.*, 9, 5389-5401, 10.5194/acp-9-5389-2009,
20 2009.

21 Morgan, W. T., Allan, J. D., Bower, K. N., Esselborn, M., Harris, B., Henzing, J. S.,
22 Highwood, E. J., Kiendler-Scharr, A., McMeeking, G. R., Mensah, A. A., Northway, M. J.,
23 Osborne, S., Williams, P. I., Krejci, R., and Coe, H.: Enhancement of the aerosol direct
24 radiative effect by semi-volatile aerosol components: airborne measurements in North-
25 Western Europe, *Atmos. Chem. Phys.*, 10, 8151-8171, 10.5194/acp-10-8151-2010, 2010a.

26 Morgan, W. T., Allan, J. D., Bower, K. N., Highwood, E. J., Liu, D., McMeeking, G. R.,
27 Northway, M. J., Williams, P. I., Krejci, R., and Coe, H.: Airborne measurements of the
28 spatial distribution of aerosol chemical composition across Europe and evolution of the
29 organic fraction, *Atmos. Chem. Phys.*, 10, 4065-4083, DOI 10.5194/acp-10-4065-2010,
30 2010b.

1 Murphy, J. G., Oram, D. E., and Reeves, C. E.: Measurements of volatile organic compounds
2 over West Africa, *Atmos. Chem. Phys.*, 10, 5281-5294, 10.5194/acp-10-5281-2010, 2010.

3 Nannoolal, Y., Rarey, J., Ramjugernath, D., and Cordes, W.: Estimation of pure component
4 properties Part 1. Estimation of the normal boiling point of non-electrolyte organic
5 compounds via group contributions and group interactions, *Fluid Phase Equilibr*, 226, 45-63,
6 DOI 10.1016/j.fluid.2004.09.001, 2004.

7 Nannoolal, Y., Rarey, J., and Ramjugernath, D.: Estimation of pure component properties -
8 Part 3. Estimation of the vapor pressure of non-electrolyte organic compounds via group
9 contributions and group interactions, *Fluid Phase Equilibr*, 269, 117-133, DOI
10 10.1016/j.fluid.2008.04.020, 2008.

11 Ng, N. L., Herndon, S. C., Trimborn, A., Canagaratna, M. R., Croteau, P. L., Onasch, T. B.,
12 Sueper, D., Worsnop, D. R., Zhang, Q., Sun, Y. L., and Jayne, J. T.: An Aerosol Chemical
13 Speciation Monitor (ACSM) for Routine Monitoring of the Composition and Mass
14 Concentrations of Ambient Aerosol, *Aerosol Sci. Technol.*, 45, 780-794,
15 10.1080/02786826.2011.560211, 2011.

16 Nguyen, T. B., Coggon, M. M., Bates, K. H., Zhang, X., Schwantes, R. H., Schilling, K. A.,
17 Loza, C. L., Flagan, R. C., Wennberg, P. O., and Seinfeld, J. H.: Organic aerosol formation
18 from the reactive uptake of isoprene epoxydiols (IEPOX) onto non-acidified inorganic seeds,
19 *Atmos. Chem. Phys.*, 14, 3497-3510, 10.5194/acp-14-3497-2014, 2014.

20 Paulot, F., Crounse, J. D., Kjaergaard, H. G., Kürten, A., St. Clair, J. M., Seinfeld, J. H., and
21 Wennberg, P. O.: Unexpected Epoxide Formation in the Gas-Phase Photooxidation of
22 Isoprene, *Science*, 325, 730-733, 10.1126/science.1172910, 2009.

23 Petzold, A., Ogren, J. A., Fiebig, M., Laj, P., Li, S. M., Baltensperger, U., Holzer-Popp, T.,
24 Kinne, S., Pappalardo, G., Sugimoto, N., Wehrli, C., Wiedensohler, A., and Zhang, X. Y.:
25 Recommendations for reporting "black carbon" measurements, *Atmos. Chem. Phys.*, 13,
26 8365-8379, 10.5194/acp-13-8365-2013, 2013.

27 Pike, R. C., Lee, J. D., Young, P. J., Carver, G. D., Yang, X., Warwick, N., Moller, S.,
28 Misztal, P., Langford, B., Stewart, D., Reeves, C. E., Hewitt, C. N., and Pyle, J. A.: NO_x and
29 O₃ above a tropical rainforest: an analysis with a global and box model, *Atmos. Chem. Phys.*,
30 10, 10607-10620, 10.5194/acp-10-10607-2010, 2010.

1 Pye, H. O. T., Pinder, R. W., Piletic, I. R., Xie, Y., Capps, S. L., Lin, Y.-H., Surratt, J. D.,
2 Zhang, Z., Gold, A., Luecken, D. J., Hutzell, W. T., Jaoui, M., Offenberg, J. H., Kleindienst,
3 T. E., Lewandowski, M., and Edney, E. O.: Epoxide Pathways Improve Model Predictions of
4 Isoprene Markers and Reveal Key Role of Acidity in Aerosol Formation, *Environ. Sci.*
5 *Technol.*, 47, 11056-11064, 10.1021/es402106h, 2013.

6 Robinson, N. H., Hamilton, J. F., Allan, J. D., Langford, B., Oram, D. E., Chen, Q., Docherty,
7 K., Farmer, D. K., Jimenez, J. L., Ward, M. W., Hewitt, C. N., Barley, M. H., Jenkin, M. E.,
8 Rickard, A. R., Martin, S. T., McFiggans, G., and Coe, H.: Evidence for a significant
9 proportion of Secondary Organic Aerosol from isoprene above a maritime tropical forest,
10 *Atmos. Chem. Phys.*, 11, 1039-1050, 10.5194/acp-11-1039-2011, 2011.

11 Robinson, N. H., Allan, J. D., Trembath, J. A., Rosenberg, P. D., Allen, G., and Coe, H.: The
12 lofting of Western Pacific regional aerosol by island thermodynamics as observed around
13 Borneo, *Atmos. Chem. Phys.*, 12, 5963-5983, DOI 10.5194/acp-12-5963-2012, 2012.

14 Slowik, J. G., Brook, J., Chang, R. Y. W., Evans, G. J., Hayden, K., Jeong, C. H., Li, S. M.,
15 Liggio, J., Liu, P. S. K., McGuire, M., Mihele, C., Sjostedt, S., Vlasenko, A., and Abbatt, J. P.
16 D.: Photochemical processing of organic aerosol at nearby continental sites: contrast between
17 urban plumes and regional aerosol, *Atmos. Chem. Phys.*, 11, 2991-3006, DOI 10.5194/acp-
18 11-2991-2011, 2011.

19 Song, M., Marcolli, C., Krieger, U. K., Lienhard, D. M., and Peter, T.: Morphologies of
20 mixed organic/inorganic/aqueous aerosol droplets, *Faraday Discuss.*, 165, 289-316,
21 10.1039/C3FD00049D, 2013.

22 Surratt, J. D., Murphy, S. M., Kroll, J. H., Ng, N. L., Hildebrandt, L., Sorooshian, A.,
23 Szmigielski, R., Vermeylen, R., Maenhaut, W., Claeys, M., Flagan, R. C., and Seinfeld, J. H.:
24 Chemical composition of secondary organic aerosol formed from the photooxidation of
25 isoprene, *J Phys Chem A*, 110, 9665-9690, Doi 10.1021/Jp061734m, 2006.

26 Surratt, J. D., Kroll, J. H., Kleindienst, T. E., Edney, E. O., Claeys, M., Sorooshian, A., Ng,
27 N. L., Offenberg, J. H., Lewandowski, M., Jaoui, M., Flagan, R. C., and Seinfeld, J. H.:
28 Evidence for organosulfates in secondary organic aerosol, *Environ. Sci. Technol.*, 41, 517-
29 527, Doi 10.1021/Es062081q, 2007a.

1 Surratt, J. D., Lewandowski, M., Offenberg, J. H., Jaoui, M., Kleindienst, T. E., Edney, E. O.,
2 and Seinfeld, J. H.: Effect of acidity on secondary organic aerosol formation from isoprene,
3 *Environ. Sci. Technol.*, 41, 5363-5369, Doi 10.1021/Es0704176, 2007b.

4 Surratt, J. D., Chan, A. W. H., Eddingsaas, N. C., Chan, M. N., Loza, C. L., Kwan, A. J.,
5 Hersey, S. P., Flagan, R. C., Wennberg, P. O., and Seinfeld, J. H.: Reactive intermediates
6 revealed in secondary organic aerosol formation from isoprene, *P Natl Acad Sci USA*, 107,
7 6640-6645, DOI 10.1073/pnas.0911114107, 2010.

8 Topping, D., Connolly, P., and McFiggans, G.: Cloud droplet number enhanced by co-
9 condensation of organic vapours, *Nature Geosci*, 6, 443-446, 10.1038/ngeo1809, 2013.

10 Trembath, J., Bart, M., and Brooke, J.: Efficiencies of Modified Rosemount Housings for
11 sampling Aerosol on a Fast Atmospheric Research Aircraft.,
12 http://www.faam.ac.uk/index.php/component/docman/doc_download/1673-inlet-efficiency,
13 FAAM Technical Note 01, 2012.

14 Ulbrich, I. M., Canagaratna, M. R., Zhang, Q., Worsnop, D. R., and Jimenez, J. L.:
15 Interpretation of organic components from positive matrix factorization of aerosol mass
16 spectrometric data, *Atmos. Chem. Phys.*, 9, 2891-2918, 2009.

17 Virtanen, A., Joutsensaari, J., Koop, T., Kannosto, J., Yli-Pirila, P., Leskinen, J., Makela, J.
18 M., Holopainen, J. K., Poschl, U., Kulmala, M., Worsnop, D. R., and Laaksonen, A.: An
19 amorphous solid state of biogenic secondary organic aerosol particles, *Nature*, 467, 824-827,
20 Doi 10.1038/Nature09455, 2010.

21 Wennberg, P.: Let's abandon the "high NOX" and "low NOX" terminology, *IGACnews*, 50,
22 2-3, 2013.

23 Whitehead, J. D., Gallagher, M. W., Dorsey, J. R., Robinson, N., Gabey, A. M., Coe, H.,
24 McFiggans, G., Flynn, M. J., Ryder, J., Nemitz, E., and Davies, F.: Aerosol fluxes and
25 dynamics within and above a tropical rainforest in South-East Asia, *Atmos. Chem. Phys.*, 10,
26 9369-9382, 10.5194/acp-10-9369-2010, 2010.

27 Zuend, A., Marcolli, C., Luo, B. P., and Peter, T.: A thermodynamic model of mixed organic-
28 inorganic aerosols to predict activity coefficients, *Atmos. Chem. Phys.*, 8, 4559-4593,
29 10.5194/acp-8-4559-2008, 2008.

1 Zuend, A., Marcolli, C., Booth, A. M., Lienhard, D. M., Soonsin, V., Krieger, U. K., Topping,
2 D. O., McFiggans, G., Peter, T., and Seinfeld, J. H.: New and extended parameterization of
3 the thermodynamic model AIOMFAC: calculation of activity coefficients for organic-
4 inorganic mixtures containing carboxyl, hydroxyl, carbonyl, ether, ester, alkenyl, alkyl, and
5 aromatic functional groups, *Atmos. Chem. Phys.*, 11, 9155-9206, 10.5194/acp-11-9155-2011,
6 2011.

7

8

9

10

1
2
3
4
5
6

Table 1: Composition statistics for the data taken below 2 km for the 5 flights, with standard deviations, shown to 3 significant digits. Time periods refer to AMS data coverage. All mass concentrations are reported at standard temperature and pressure (273.15 K, 1013 hPa). Quantities denoted by * were impacted by an inlet blockage and failed quantification quality checks.

Flight	B735	B744	B745	B749	B750
Date and time (UTC-4)	19 Sep 2012 07:59-11:48	28 Sep 2012 08:50-12:44	28 Sep 2012 13:58-17:07	03 Oct 2012 09:33-13:30	03 Oct 2012 14:57-17:35
Region	Amazon (Manaus)	Pacaás Novos	Pacaás Novos	Amazon (Porto Velho)	Amazon (Porto Velho)
Org _{Total} ($\mu\text{g m}^{-3}$)	0.614* 0.275	$\pm 5.46 \pm 1.94$	5.53 ± 1.74	3.36 ± 1.16	2.41 ± 1.03
Org ₈₂ (ng m^{-3})	$5.49^* \pm 3.29$	22.1 ± 8.0	22.2 ± 6.4	28.5 ± 10.2	22.4 ± 9.3
SO ₄ ²⁻ (ng m^{-3})	$137^* \pm 55$	484 ± 163	451 ± 65	425 ± 139	327 ± 104
NO ₃ ⁻ (ng m^{-3})	$29.8^* \pm 31.6$	261 ± 167	232 ± 241	137 ± 69	97.7 ± 72.7
NH ₄ ⁺ (ng m^{-3})	$12.3^* \pm 59.4$	242 ± 154	212 ± 135	110 ± 96	41.8 ± 84.7
rBC (ng m^{-3})	582 ± 258	434 ± 144	463 ± 148	371 ± 61	259 ± 67
Isoprene (ppbv)	3.58 ± 2.32	0.62 ± 1.02	1.44 ± 1.51	4.77 ± 1.98	1.81 ± 1.49
NO (pptv)	11.9 ± 7.8	28.9 ± 12.0	35.7 ± 51.1	19.0 ± 8.9	8.84 ± 8.07
NO ₂ (pptv)	64.3 ± 31.1	174 ± 44	256 ± 194	47.5 ± 24.8	119 ± 37

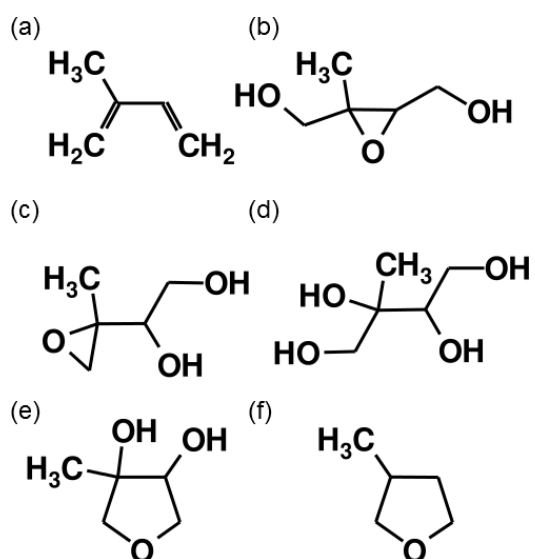
7
8

1 Table 2: Diagnostic ratios for the five flights. All ratios are slopes from linear regressions
2 (with intercepts fixed at 0) with associated uncertainties, except $\text{Org}_{82}/\text{Org}_{\text{Total}}$, which is a
3 ratio of means with associated standard error, for the sake of comparability with Robinson et
4 al. (2011), although due to the high degree of correlation, slopes from linear regressions were
5 numerically very similar. With M_{30}/M_{46} , M_{46} was treated as the dependent variable due to its
6 lower signal-to-noise.

Flight	B735	B744	B745	B749	B750	
$r^2_{\text{Org},82}$	0.2129	0.867	0.856	0.795	0.831	
$\text{Org}_{82}/\text{Org}_{\text{Total}}$ (‰)	8.94 ± 0.23	4.05 ± 0.03	4.01 ± 0.02	8.48 ± 0.07	9.30 ± 0.08	
M_{30}/M_{46}	7.74 ± 1.25	1.83 ± 0.02	2.27 ± 0.02	4.07 ± 0.11	5.75 ± 0.15	
$\text{NH}_4^+/\text{NH}_4^+_{\text{Neut}}$	0.277 0.040	$\pm 1.05 \pm 0.019$	0.913 0.015	± 0.601 0.016	± 0.321 0.022	\pm
$\text{NH}_4^+/\text{NH}_4^+_{\text{SO}_4}$	0.316 0.048	$\pm 1.56 \pm 0.03$	1.42 ± 0.03	0.783 0.022	± 0.404 0.029	\pm
$r^2_{\text{Org},\text{rBC}}$	0.490	0.754	0.386	0.329	0.561	

7

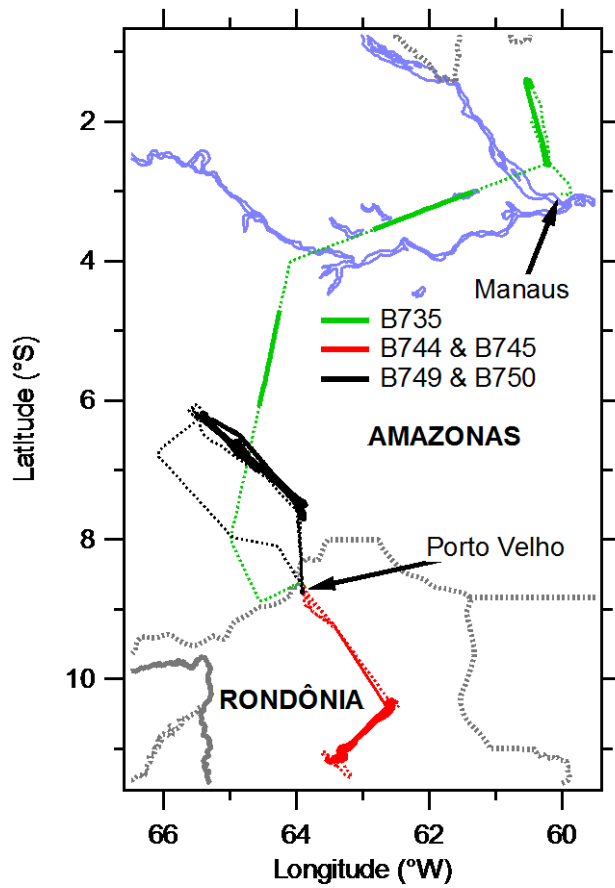
8



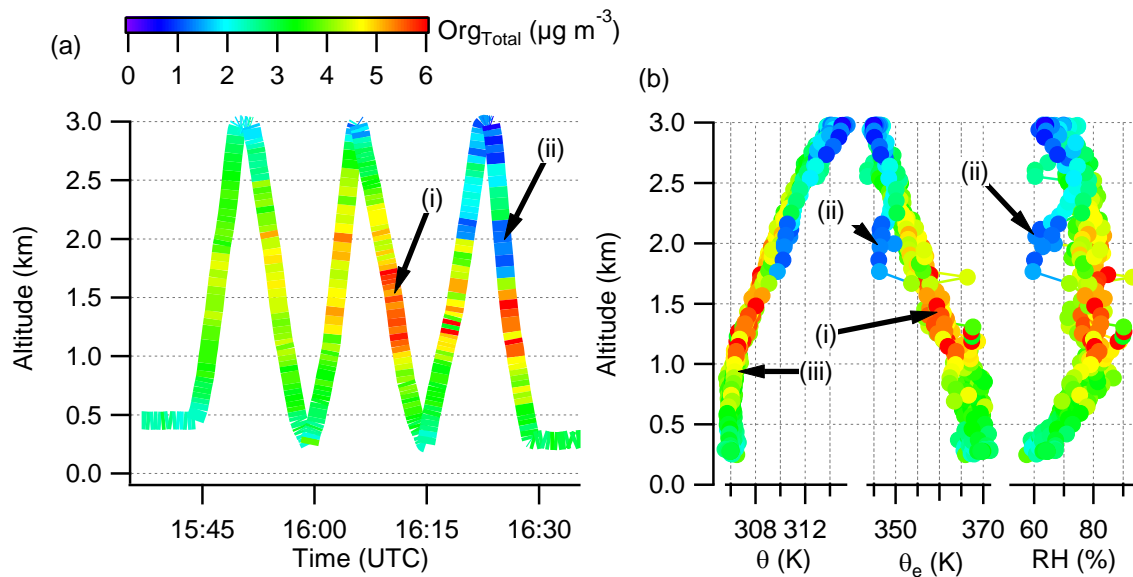
1

2 Figure 1: Organic species referred to in this manuscript: (a) Isoprene, (b) β -IEPOX, (c) δ -
 3 IEPOX, (d) 2-methyltetrol, (e) 3-methyltetrahydrofuran-3,4-diol and (f) 3-methylfuran

4



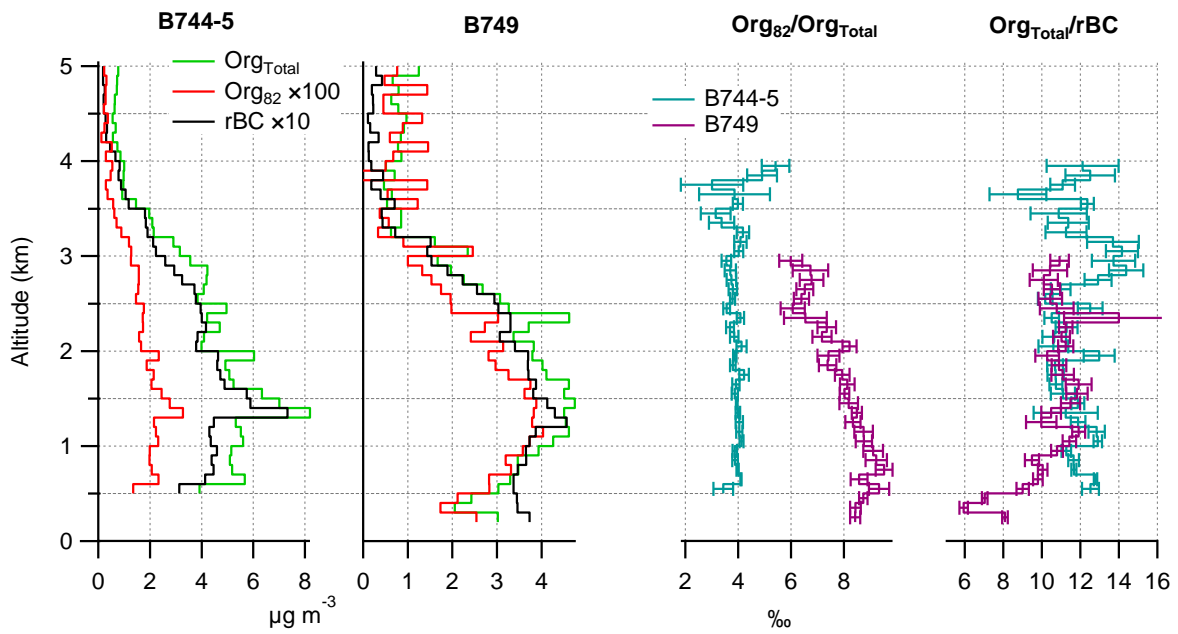
1
 2 Figure 2: Tracks of the flights presented in this article. The portions of the flights used in
 3 generating the statistics in Tables 1 and 2 (altitude below 2 km, excluding takeoffs, landings
 4 and approaches) are shown as solid lines, with the rest of the flights dotted.
 5



1

2 Figure 3: Profile data of potential temperature (θ), equivalent potential temperature (θ_e) and
 3 relative humidity (RH) from the B749 'sawtooth' manoeuvre, coloured according to organic
 4 mass concentration. Highlighted are the (i) peak in organic concentration, (ii) layer of low
 5 mass concentration and humidity and (iii) top of the well-mixed boundary layer, as evidenced
 6 by θ .

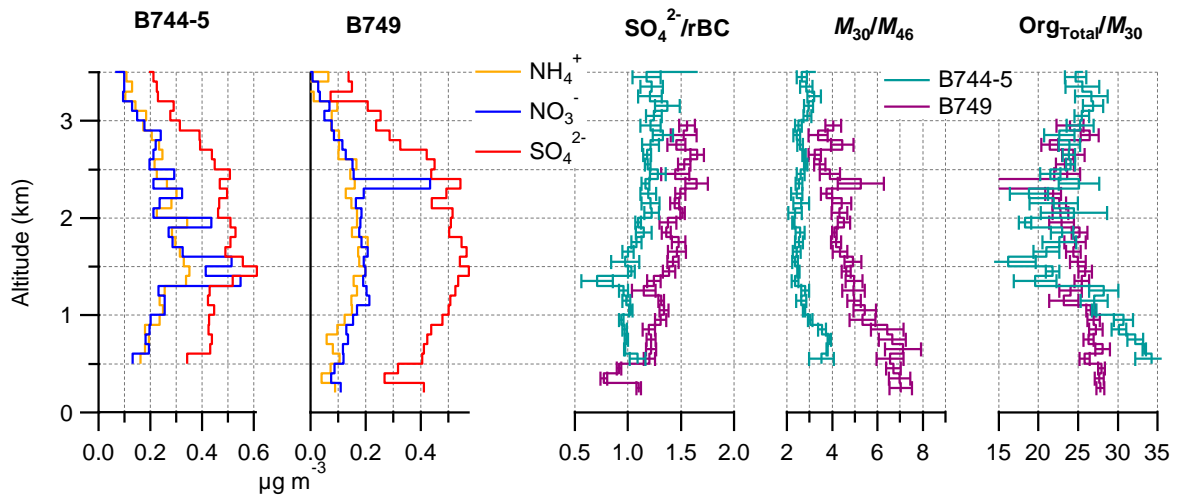
7



1

2 Figure 4: Comparison of mean vertical profiles of B744 and B745 with B749 for the
 3 carbonaceous species. The ratios are taken of the average values and the error bars correspond
 4 to standard errors. Ratios for higher altitudes showed high degree of variability (and
 5 associated errors) and have been omitted for clarity.

6

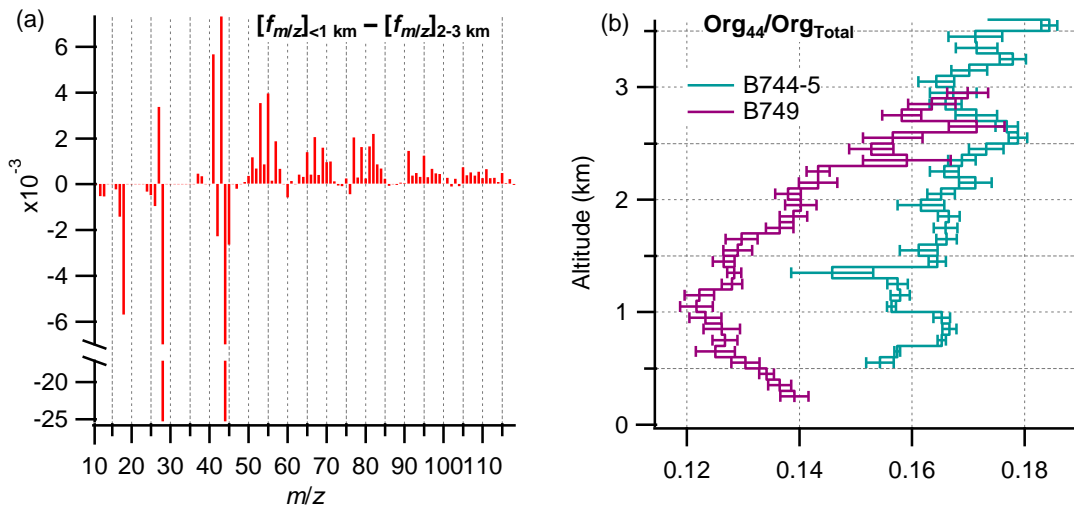


1

2 Figure 5: Inorganic vertical profiles for B744-5 and B749. Data above 3.5 km are omitted for
 3 clarity.

4 .

5



1

2 Figure 6: (a) Difference in normalised organic mass spectra between the altitude ranges of
 3 less than 1 km and between 2 and 3 km. (b) Trend in $\text{Org}_{44}/\text{Org}_{\text{Total}}$ with altitude for the two
 4 contrasting cases, with standard errors.

5